C^{3}DA: A Universal Domain Adaptation Method for Scene Classification From Remote Sensing Imagery

Jiaxu Guo, *Graduate Student Member, IEEE*, Yushan Lai, Jinxiao Zhang, Juepeng Zheng, Haohuan Fu, *Senior Member, IEEE*, Lin Gan, *Member, IEEE*, Liang Hu, Gaochao Xu, and Xilong Che

***Abstract*— Various remote sensing applications have widely used domain adaptation (DA) methods. Since it does not need to add human interpretation in the target domain, it can be used in cross-region, multitemporal, and multisensor application scenarios. In order to further optimize the design of the loss function and better address the challenges of DA in remote sensing, in this letter, we propose a new universal DA method named C^{3}DA for scene recognition of remote sensing images. It has a comprehensive C^3 criterion for recognizing the "unknown" classes by innovatively fusing confidence, consistency, and certainty of samples to make our network training more efficient. We evaluate the performance of our proposed method based on six transfer tasks on three remote sensing datasets. The evaluation results show that our proposed method achieves an average *H*-score of 58.44%, significantly higher than other SOTA universal DA methods with an average improvement of 2.32%∼29.43%. Compared to the baseline ResNet-50, it achieves up to 19.92% improvement, demonstrating that the proposed method outperforms the universal DA scenario. In the future, we also plan to expand the application of this method to more scenarios.**

***Index Terms*— Deep learning, remote sensing, scene classification, universal domain adaptation (DA).**

Manuscript received 25 January 2024; revised 19 March 2024; accepted 26 March 2024. Date of publication 29 March 2024; date of current version 5 April 2024. This work was supported in part by the National Natural Science Foundation of China under Grant T2125006, in part by Jiangsu Innovation Capacity Building Program under Grant BM2022028, and in part by the National Key Research and Development Plan of China under Grant 2017YFA0604500. *(Corresponding author: Juepeng Zheng.)*

Jiaxu Guo is with the College of Computer Science and Technology, Jilin University, Changchun 130012, China, and also with the National Supercomputing Center in Wuxi, Wuxi 214071, China (e-mail: jllsgjx@yeah.net).

Yushan Lai and Juepeng Zheng are with the School of Artificial Intelligence, Sun Yat-sen University, Zhuhai 519082, China (e-mail: laiysh6@mail2.sysu.edu.cn; zhengjp8@mail.sysu.edu.cn).

Jinxiao Zhang is with the Department of Earth System Science, Tsinghua University, Beijing 100190, China (e-mail: zhang-jx22@mails.tsinghua.edu.cn).

Haohuan Fu is with Tsinghua Shenzhen International Graduate School, Tsinghua University, Shenzhen 518071, China, also with the Ministry of Education Key Laboratory for Earth System Modeling and the Department of Earth System Science, Tsinghua University, Beijing 100190, China, and also with the National Supercomputing Center in Wuxi, Wuxi 214071, China (e-mail: haohuan@tsinghua.edu.cn).

Lin Gan is with the Department of Computer Science and Technology, Tsinghua University, Beijing 100190, China, and also with the National Supercomputing Center in Wuxi, Wuxi 214071, China (e-mail: lingan@tsinghua.edu.cn).

Liang Hu, Gaochao Xu, and Xilong Che are with the College of Computer Science and Technology, Jilin University, Changchun 130012, China (e-mail: hul@jlu.edu.cn; xugc@jlu.edu.cn; chexilong@jlu.edu.cn).

Digital Object Identifier 10.1109/LGRS.2024.3383061

I. Introduction

REMOTE sensing can obtain accurate and objective geographic information quickly and timely. As a remote sensing image, it can accurately and vividly depict the current distribution of surface features, the relationships between them, and the mutual interactions and changes among them [1]. The introduction of remote sensing technology has provided convenience and a foundation for in-depth research on regional geographic comprehensive dynamic analysis and has improved the practical value and benefit of the results [2], [3]. In the classification of remote sensing images, phenomena such as variations in spectral signatures of the same object and similarities in spectral signatures of different objects occur frequently [4]. Due to differences in geographical location, environment, and seasonal changes, the form of the same ground object on the image may not be the same. Conversely, what appears to be the same in the image may not necessarily represent the same object or phenomenon. These aforementioned issues can introduce complexity to the interpretation of remote sensing images, necessitating the utilization of deep learning methods to achieve more accurate classification [5].

In this scenario, domain adaptation (DA) provides great potential to improve the generalization ability of deep learning models and is becoming a widely-used strategy for transfer learning [6]. According to the inclusion relationship of sample labels between the source and target domains, DA can be archived into four categories [7]. Closed-set DA refers to the situation where the classes contained in the source and target domains are identical [Fig. 1(a)]. Partial DA refers to a scenario where the classes present in the target domain are a subset of the classes found in the source domain [8], indicating the presence of outlier classes in the source domain [Fig. 1(b)]. In contrast, open-set DA describes a situation where the classes present in the source domain form a subset of the classes in the target domain, resulting in the presence of "unknown" classes in the target domain [Fig. 1(c)]. Furthermore, universal DA generalizes the three aforementioned DA settings. It defines a scenario where the source and target domains typically share some labels but each also has a unique set of labels not found in the other, without being constrained by prior knowledge [Fig. 1(d)] [9], [10].

In deep learning and computer vision, the design of the loss function holds significant importance [11]. The training process of a model involves optimizing the loss function to adjust the model parameters. In the case of universal DA in remote sensing imagery, the principle remains consistent.

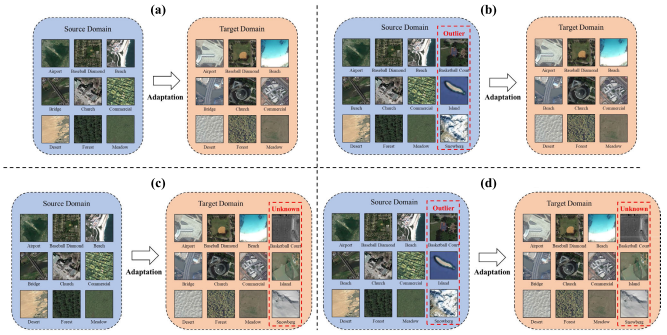

Fig. 1. Some examples of four typical cases of DA. (a) Standard domain adaptation ($C_t \equiv C_s$). (b) Partial domain adaptation ($C_t \subseteq C_s$). (c) Open-set domain adaptation ($C_t \supseteq C_s$). (d) Universal domain adaptation.

Enhanced design of loss functions contributes significantly to improving the classification performance of remote sensing images. Particularly within the realm of universal DA, given the distinctive characteristics of remote sensing images, the identification of unknown classes presents a significant challenge. Currently, further exploration into the research of loss functions in remote sensing image classification is warranted.

In this letter, we propose a novel universal DA method named C^{3}DA for the classification of remote sensing images. The main contributions of it can be summarized in the following points.

1) We propose a comprehensive C^3 criterion to better recognize the "unknown" classes in remote sensing images.
2) Our proposed C^{3}DA method with a two-stage (TS) attention mechanism can better minimize the negative effect from outlier classes in the source domain.
3) The evaluation results of six tasks for three datasets show that our C^{3}DA method attains a 19.92% gain compared to baseline and yields 2.32%∼29.43% improvements compared to other universal DA methods.

II. Methodology

A. Preliminary

In the universal DA scenario, we define the dataset of the source domain as $(D_s = \{(\mathbf{x}_i^s, y_i^s)\}_{i=1}^{n_s})$, where the images are labeled. Correspondingly, the dataset of the target domain is $(D_t = \{(\mathbf{x}_i^t)\}_{i=1}^{n_t})$, the images in it are not yet labeled. In the above definition, n_s and n_t are the number of images in the two datasets, respectively. D_s and D_t are sampled from different distributions. We assume that C_s and C_t represent the label sets of the source and target domains. Let $C_c = C_s \cap C_t$ denote the set of labels common to the above two domains. $\overline{C}_s = C_s \backslash C_c$ represents the set of labels that are private in the source domain, and $\overline{C}_t = C_t \backslash C_c$ correspondingly represents the set of labels that are private in the target domain. The overall goal of adaptation is to identify target samples with either one of the "known" common labels (C_c) or the "unknown" label ($\overline{C}_t$) based on labeled $\mathcal{D}_s$ and unlabeled $\mathcal{D}_t$.

B. Network Architecture

Fig. 2 depicts the framework of C^{3}DA, it consists of the following parts, including feature extractor $\mathcal{F}$, multiple classifiers $\mathcal{G}_i|_{i=1}^m$ and domain discriminator $\mathcal{D}$. In the meantime, our proposed C^{3}DA has a comprehensive C^3 criterion for recognizing "unknown" classes fusing confidence, consistency, and

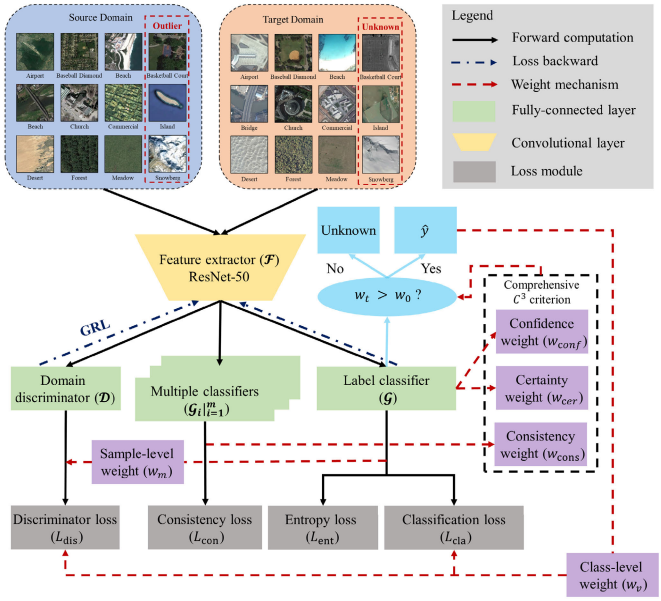

Fig. 2. Overall framework for our proposed C^{3}DA, including feature extractor $\mathcal{F}$, multiple classifiers $\mathcal{G}_i|_{i=1}^m$ and domain discriminator $\mathcal{D}$.

certainty of samples to make network training more efficient, as well as to achieve higher classification performance for universal DA scenario.

We adopt adversarial learning to align feature representations by incorporating classification from the source domain with gradient reversal layer (GRL) [12] to make $\mathcal{D}$ indistinguishable whether the sample that comes from either of the two domains, which is the well-established domain adversarial neural network (DANN) and their loss can be calculated as

$$\begin{aligned} C_{\text{DANN}}(\theta_f, \theta_y, \theta_d) &= C_{\text{cls}}(\theta_f, \theta_y) - \lambda C_{\text{adv}}(\theta_f, \theta_d) \\ &= \frac{1}{n_s} \sum_{\mathbf{x}_i \in D_s} L_{\text{cla}}(\mathcal{G}(\mathcal{F}(\mathbf{x}_i)), y_i) \\ &\quad - \frac{\lambda}{n} \sum_{\mathbf{x}_i \in D_s \cup D_t} L_{\text{dis}}(\mathcal{D}(\mathcal{F}(\mathbf{x}_i)), d_i) \quad (1) \end{aligned}$$

where $n = n_s + n_t$, and λ is a hyper-parameter used to balance the classification loss (L_{cla}) and domain loss (L_{dis}).

1) TS Attention Mechanism: In universal DA, classes that exist only in the source domain are called outlier classes. Their presence would have serious negative transfer effects and make the model perform worse [9]. To better solve this problem, we introduce a TS attention mechanism to improve the existing DANN.

This mechanism consists of two weights, including entropy-aware and target-class-aware [13]. In (1), it is implausible that each sample from both domains performs identically in L_d. These samples with uncertain predictions are difficult to transfer, and they may cause deterioration in the adversarial learning process. Therefore, we use the entropy criterion to quantitatively analyze the uncertainty in the prediction, as follows: $H(\hat{\mathbf{y}}) = -\sum_{c=1}^{C} \hat{y}_c \log(\hat{y}_c)$, where C is the number of classes and $\hat{y}_c$ is the predicted probability that a sample belongs to class c. Therefore, with an entropy-aware weight $w_m(\mathbf{x}_i) = 1 + e^{-H(\mathcal{G}(\mathcal{F}(\mathbf{x}_i)))}$, we can re-weight the $\mathcal{D}$ by each training sample. It is worth noting that w_m is the sample-level weight.

On the other hand, we also utilize a simple re-weighting mechanism to decrease the contribution of the samples belonging to the outlier classes. We take the average of the predictions $\hat{\mathbf{y}}$ of all samples in the target domain, which can effectively minimize the impact of the outlier classes. To that end, the weight vector could be calculated as $\mathbf{w}_v = (1/n_t)\sum_{i=1}^{n_t}\hat{\mathbf{y}}_i$, where $\mathbf{w}_v$ is a class-level weight vector with $|\mathcal{C}_s|$-dimension. The improved adversarial learning objective is shown in (2), and the classification objective is shown in (3)

$$C_{\text{adv}}(\theta_f,\theta_d) = \frac{1}{n_s}\sum_{\mathbf{x}_i\in\mathcal{D}_s} w_v^{y_i} w_m(\mathbf{x}_i) L_d(\mathcal{D}(\mathcal{F}(\mathbf{x}_i)),1) + \frac{1}{n_t}\sum_{\mathbf{x}_i\in\mathcal{D}_t} w_m(\mathbf{x}_i) L_d(\mathcal{D}(\mathcal{F}(\mathbf{x}_i)),0) \tag{2}$$

$$C_{\text{cls}}(\theta_f,\theta_y) = \frac{1}{n_s}\sum_{\mathbf{x}_i\in\mathcal{D}_s} w_v^{y_i} L_y(\mathcal{G}(\mathcal{F}(\mathbf{x}_i)),y_i) \tag{3}$$

where θ_f, θ_y, and θ_d are the parameters of networks.

However, in a universal DA scenario, another challenge is that there may exist "unknown" classes. Here we introduce a comprehensive C³ criterion to better recognize the open classes.

2) Comprehensive "C³" Criterion:

a) Certainty: In general, entropy is used to measure the certainty of the predicted class distribution [5]. We use the entropy criterion to quantitatively analyze the uncertainty in the prediction as $H(\hat{\mathbf{y}}^t) = -\sum_{c=1}^{C}\hat{y}_c^t\log(\hat{y}_c^t)$, which is the same as Section II-B1. In general, the sample in $\overline{C}_t$ usually has higher entropy and lower certainty, while the sample in C usually has lower entropy and higher certainty.

However, recognizing "unknown" classes only by certainty will fail to discriminate uncertain and extremely sharp predictions, especially when the number of classes is large [14]. Therefore, we introduce two other criteria, confidence, and consistency, to decide the "unknown" classes jointly.

b) Confidence: Confidence is qualified as the highest value among predicted probabilities, which is higher for a more certain sample in the common class (C). Some universal DA methods adopt confidence to decide the "unknown" samples [7]. However, it may fail to recognize actual "unknown" classes only depending on the confidence criterion. Although the confidence of different class distributions is the same, the degrees of certainty vary. This also suggests that high-confidence yet low-certainty samples will diminish the model's ability to effectively recognize "unknown" classes [15]. Therefore, we jointly fuse certainty and the following consistency to recognize the "unknown" classes.

c) Consistency: The certainty and confidence jointly address smooth and nonsmooth class distributions to recognize open class samples better. However, confidence sometimes will suffer from incorrect predictions. For example, if the classifier predicts an "unknown" sample as a class in C with high confidence, the confidence will mistakenly select this sample as a shared class sample, which is wrong. To this end, we add another criterion, consistency, that is built on multiple classifiers $(\mathcal{G}_i|_{i=1}^m)$, which indicates the agreement of different classifiers. Consistency is more robust for error predictions because the probability that all classifiers are wrongly and coincidentally into the same class is low, which means all multiple classifiers make the same mistake. Therefore, consistency is compensative for confidence and certainty for prediction errors.

In order to jointly make full use of the respective advantages of the above three criteria, we propose a new "C³" criterion that fuses them to better recognize "unknown" classes in a universal DA scenario. We calculate the certainty w_{cer}, confidence w_{conf} and consistency w_{cons} as follows:

$$w_{\text{cer}} = \sum_{j=1}^{|C|} -\hat{y}_j^t\log(\hat{y}_j^t) \tag{4}$$

$$w_{\text{conf}} = \max(\hat{\mathbf{y}}^t) \tag{5}$$

$$w_{\text{cons}} = \frac{1}{|C|}\left\|\hat{\mathbf{y}}^t - \frac{1}{m}\sum_{i=1}^{m}\hat{\mathbf{y}}_i^t\right\| \tag{6}$$

where $\hat{y}_j^t$ denotes predicted probability of jth class in common classes (C) and m is the number of multiple classifiers. We calculate the "C³" criterion w_t by fusing three criteria

$$w_t = \frac{1}{3}[(1-w_{\text{cer}}) + w_{\text{conf}} + (1-w_{\text{cons}})] \tag{7}$$

in which higher $w_t(\mathbf{x}^t)$ denotes that $\mathbf{x}^t$ is more likely in common classes (C). In addition, w_{cer} and w_{cons} are normalized by min-max normalization.

3) Overall Objective: After integrating the above three criteria, our proposed C³DA contains a TS-weight-aware DANN and an attentive entropy regularization. In summary, the final learning objective can be formulated as follows:

$$\begin{aligned} C_{\text{C}^3\text{DA}}(\theta_f,\theta_y,\theta_d) &= C_{\text{cls}}(\theta_f,\theta_y) - \lambda C_{\text{adv}}(\theta_f,\theta_d) + \alpha C_{\text{ent}}(\theta_f,\theta_y,\theta_d) \\ &= \frac{1}{n_s}\sum_{\mathbf{x}_i\in\mathcal{D}_s} w_v^{y_i} L_y(\mathcal{G}(\mathcal{F}(\mathbf{x}_i)),y_i) \\ &\quad -\frac{\lambda}{n_s}\sum_{\mathbf{x}_i\in\mathcal{D}_s} w_v^{y_i} w_m(\mathbf{x}_i) L_d(\mathcal{D}(\mathcal{F}(\mathbf{x}_i)),1) \\ &\quad -\frac{\lambda}{n_t}\sum_{\mathbf{x}_i\in\mathcal{D}_t} w_m(\mathbf{x}_i) L_d(\mathcal{D}(\mathcal{F}(\mathbf{x}_i)),0) \\ &\quad +\frac{\alpha}{n}\sum_{\mathbf{x}_i\in\mathcal{D}_s\cup\mathcal{D}_t}\sum_{c=1}^{C} w_m^c(\mathbf{x}_i)\cdot\hat{y}_{i,c}\cdot\log(\hat{y}_{i,c}) \end{aligned} \tag{8}$$

in which C_{cls}, C_{adv} and C_{ent} denote the learning objective of the classification for samples from the source domain, the domain discriminator and the attentive entropy objective. λ and α are the hyper-parameters that trade off the domain discriminator and attentive entropy objective with the classification objective in the unified optimization, respectively. The optimization of min-max issue in (8) is aiming to find the network parameters θ_f, θ_y, and θ_d that consistently satisfy as following:

$$\begin{aligned} (\hat{\theta}_f,\hat{\theta}_y) &= \arg\min_{\theta_f,\theta_y} C_{\text{C}^3\text{DA}}(\theta_f,\theta_y) \\ (\hat{\theta}_d) &= \arg\max_{\theta_d} C_{\text{C}^3\text{DA}}(\theta_d). \end{aligned} \tag{9}$$

In the inference stage, we first calculate $w_t(\mathbf{x}_t)$ for a given target sample $(\mathbf{x}_t)$ and then predict the class with the threshold w_0 as follows:

$$y(\mathbf{x}^t) = \begin{cases} \text{unknown}, & w_t(\mathbf{x}^t) \le w_0 \\ \text{argmax}(\hat{\mathbf{y}}^t), & w_t(\mathbf{x}^t) > w_0. \end{cases} \tag{10}$$

TABLE I

LABELS OF THE SOURCE AND TARGET DOMAINS THAT ARE PRIVATE TO EACH OF THE SIX TRANSFER TASKS AND THE TYPE OF EACH TASK

Source	Target	Private Classes in Source Domain	Private Classes in Target Domain	Type of Task
A	**N**	Bare land, Pond, Park, Center, Square, Resort, School	Basketball court, Runway, Tennis court, Intersection, Chaparral, Snowberg, Roundabout, Lake, Island, Freeway, Cloud, Wetland, Sea ice, Palace, Terrace, Golf course, Thermal power station, Airplane, Ship, Mobile home park	**Universal DA**
A	**U**	Meadow, Bare land, Desert, Square, Stadium, Center, Church, Bridge, School, Mountain, Desert, Industrial, Airport, Railway station	Airplane, Chaparral, Golf course, Mobile home park, Tennis court, Intersection, Runway, Freeway	**Universal DA**
N	**A**	Basketball court, Runway, Tennis court, Intersection, Chaparral, Snowberg, Roundabout, Lake, Island, Freeway, Cloud, Wetland, Sea ice, Palace, Terrace, Golf course, Thermal power station, Airplane, Ship, Mobile home park	Bare land, Pond, Park, Center, Square, Resort, School	**Universal DA**
N	**U**	Airport, Basketball court, Mountain, Ship, Island, Lake, Cloud, Desert, Ground track field, Industrial area, Meadow, Bridge, Palace, Railway, Railway station, Sea ice, Church, Snowberg, Stadium, Terrace, Wetland, Roundabout, Thermal power station	*None*	**Partial DA**
U	**A**	Airplane, Chaparral, Golf course, Mobile home park, Tennis court, Intersection, Runway, Freeway	Meadow, Bare land, Desert, Square, Stadium, Center, Church, Bridge, School, Mountain, Park, Playground, Pond, Resort, Desert, Industrial, Airport, Railway station	**Universal DA**
U	**N**	*None*	Airplane, Baseball diamond, Ship, Mountain, Commercial area, Cloud, Desert, Ground track field, Industrial area, Meadow, Chaparral, Palace, Railway, Railway station, Sea ice, Beach, Snowberg, Stadium, Terrace, Wetland, Roundabout, Thermal power station	**Open-set DA**

TABLE II

ACCURACY (ACC) AND H-SCORE (H-S) (%) ON OUR COLLECTED DATASET FOR UNIVERSAL DA SCENARIOS (RESNET-50)

Method		A → N		A → U		N → A		N → U		U → A		U → N		Avg	
		Acc	H-s	Acc	H-s	Acc	H-s	Acc	H-s	Acc	H-s	Acc	H-s	Acc	H-s
ResNet-50 [16]		67.66	35.23	49.46	44.74	73.09	45.64	41.14	52.75	23.00	40.33	43.98	54.07	38.52
Standard DA	DAN [17]	65.41	36.74	40.46	42.62	53.48	50.78	53.62	51.54	40.23	50.76	49.72	52.55	44.02
	DANN [12]	47.20	48.87	43.61	30.05	66.29	44.90	37.71	45.57	41.14	67.62	52.19	51.33	43.43
	JAN [18]	55.82	30.90	48.34	36.47	65.87	45.53	43.10	51.88	38.34	55.52	60.38	53.42	42.32
	CDAN [19]	48.40	50.59	30.29	35.38	61.72	50.14	39.62	50.15	23.49	49.67	61.28	46.64	44.18
Universal DA	UAN [20]	60.83	20.96	37.42	27.93	31.93	6.90	20.52	49.89	17.97	59.48	71.29	43.35	29.01
	CMU [14]	56.49	40.41	42.29	36.45	69.76	53.14	54.86	53.73	35.62	64.62	71.38	56.96	47.40
	DANCE [21]	57.84	17.51	39.14	**46.61**	64.37	22.58	54.52	54.29	52.90	63.14	71.08	55.55	42.13
	OVANet [22]	43.73	55.12	36.77	45.11	47.65	59.17	37.57	42.64	50.44	54.52	58.61	43.81	53.32
	UniOT [23]	57.67	**63.22**	33.31	42.05	**73.46**	61.36	52.14	54.55	55.31	58.08	58.65	54.87	56.12
	UniDA [7]	**64.97**	44.51	45.31	46.07	64.92	52.34	52.72	54.64	**57.76**	56.03	70.45	56.88	54.23
	C^3DA (**Ours**)	60.13	59.68	**51.57**	45.70	65.74	**64.07**	**55.33**	**55.97**	50.91	**70.71**	**73.16**	**58.81**	**58.44**

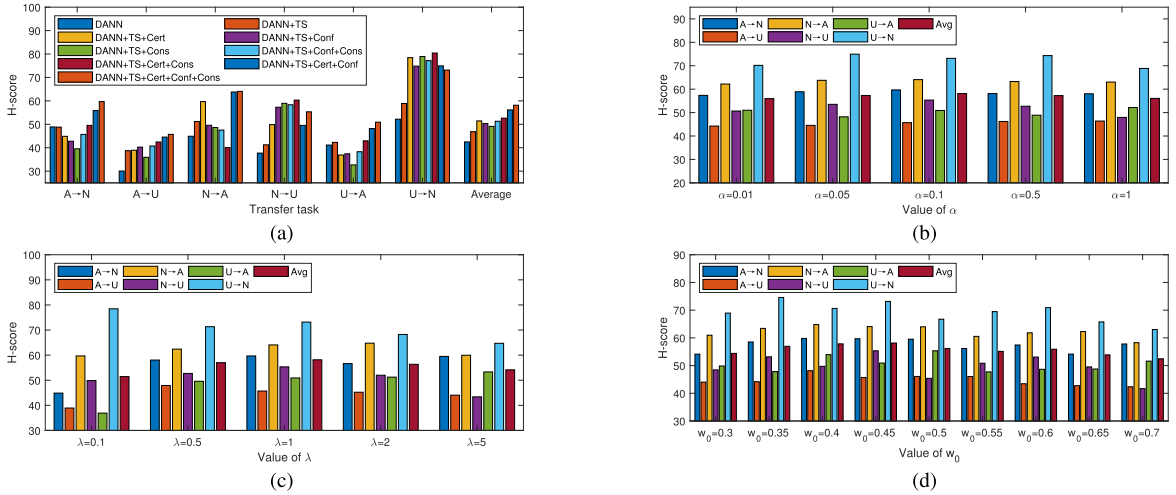

Fig. 3. Ablation experiments based on the three criteria included in C^3, as well as sensitivity experiments for α, λ, and w_0. Since N → U belongs to partial DA, the accuracy is used as the metric. (a) Ablation experiments based on C^3. (b) Sensitivity experiments for α. (c) Sensitivity experiments for λ. (d) Sensitivity experiments for w_0.

III. DATASETS

To verify the effectiveness and reliability of the proposed method while maintaining the generality of the existing methods, in this letter, we use the following three remote sensing image datasets to build transfer learning tasks: AID (**A**) [24], NWPU-RESISC45 (**N**) [25], and UC Merced (**U**) [26]. Based on these three datasets, six transfer tasks can be established. The two domain-specific classes in each task are shown in Table I. It's worth noting that the labels in the two domains may not have exactly the same name, for example, the Farmland in **A** includes both Circular farmland and Rectangular farmland in **N**. In addition, since all the classes in **U** are included in **N**, the task of **U** → **N** is actually an open-set DA task. Meanwhile, the task of **N** → **U** is actually a partial DA task. We still retain these two tasks to prove that C^{3}DA can not only improve the performance of universal DA, but also has good performance in partial and open-set DA, reflecting generality.

IV. EXPERIMENTS

A. Setup

In terms of experimental configuration, for each hyperparameter, we set $\alpha = 0.1$, $\lambda = 1.0$ and $w_0 = 0.45$. The above values are also the optimal solutions obtained through sensitivity experiments. For each transfer task, we used accuracy to evaluate the performance of the methods and averaged each method over the six tasks. In order to better characterize the classification performance of the model, we adopt H-score to jointly evaluate the accuracy on common classes (a_C) and the accuracy on target private classes ($a_{\overline{C}_t}$), which can be computed as: $H_{\text{score}} = 2 \times (a_C \times a_{\overline{C}_t})/(a_C + a_{\overline{C}_t})$.

B. Results of C³DA Criterion

In this section, our proposed method is compared with the performance of the backbone [16], four standard DA methods, and six universal DA methods on the above tasks. The baseline backbone model exclusively utilizes ResNet-50. Moreover, it is trained solely on the source domain without any involvement in DA, thus constituting a straightforward CNN model.

As can be seen from the results shown in Table II, our proposed C³DA method outperforms the comparison methods in at least one of the accuracy and H-score metrics on most tasks in the task. In general, it achieves an average accuracy of 58.81%, which is the highest among the various methods. Likewise, it has the highest average H-score of 58.44%. It achieves 1.85%∼15.46% and 2.32%∼29.43% improvement in these two metrics, which shows superior performance on most of the tasks.

Also, our proposed method attains 4.74% and 19.92% gains for accuracy and H-score compared to the straightforward CNN model. In addition, for the partial DA scenario ($\mathbf{N} \rightarrow \mathbf{U}$) and the open-set DA scenario ($\mathbf{U} \rightarrow \mathbf{N}$), it also achieves the best performance. This fully reflects the generality of C³DA proposed in this letter, it has excellent performance in various DA scenarios.

C. Ablation Study and Sensitivity Analysis

In order to fully analyze the impact of C³ criterion and hyperparameters on classification results, we conducted ablation experiments and sensitivity analyses. Fig. 3(a) presents the ablation experiment results for the C³ criterion. In terms of the average performance on the six transfer tasks, applying all three criteria simultaneously outperforms using one or two criteria. Meanwhile, Fig. 3(b)–(d) present the results of sensitivity tests for three parameters: α, λ, and w_0. From the average performance of the six transfer tasks, the best overall performance can be obtained when $\alpha = 0.1$, $\lambda = 1.0$, and $w_0 = 0.45$.

V. Conclusion

In this letter, we propose a new universal DA method called C³DA for scene classification in remote sensing imagery, which tackles the problem that we do not have any prior knowledge of the labels in the source and target domains. Our proposed C³DA has an ensemble criterion for "unknown" classes fusing confidence, consistency, and certainty of samples to make our network training more efficient and achieve higher performance under a universal DA scenario.

Results show that our proposed method can better solve problems in practice. It has higher versatility and can save more on labor costs for labeling. In the long run, this will help us to better analyze remote sensing images and, thus, better develop and utilize land resources.

References

[1] Q. Xu, Y. Shi, and X. Zhu, "Universal domain adaptation without source data for remote sensing image scene classification," in *Proc. IEEE Int. Geosci. Remote Sens. Symp. (IGARSS)*, Jul. 2022, pp. 5341–5344.

[2] Y. Zhang, M. Zhang, W. Li, S. Wang, and R. Tao, "Language-aware domain generalization network for cross-scene hyperspectral image classification," *IEEE Trans. Geosci. Remote Sens.*, vol. 61, pp. 1–12, 2023.

[3] J. Guo et al., "GEO-WMS: An improved approach to geoscientific workflow management system on HPC," *CCF Trans. High Perform. Comput.*, vol. 5, no. 4, pp. 360–373, Dec. 2023.

[4] Y. Zhang, W. Li, W. Sun, R. Tao, and Q. Du, "Single-source domain expansion network for cross-scene hyperspectral image classification," *IEEE Trans. Image Process.*, vol. 32, pp. 1498–1512, 2023.

[5] Y. Zhang, W. Li, M. Zhang, S. Wang, R. Tao, and Q. Du, "Graph information aggregation cross-domain few-shot learning for hyperspectral image classification," *IEEE Trans. Neural Netw. Learn. Syst.*, vol. 35, no. 2, pp. 1912–1925, Feb. 2024.

[6] J. Zheng, W. Wu, S. Yuan, H. Fu, W. Li, and L. Yu, "Multisource-domain generalization-based oil palm tree detection using very-high-resolution (VHR) satellite images," *IEEE Geosci. Remote Sens. Lett.*, vol. 19, pp. 1–5, 2022.

[7] Q. Xu, Y. Shi, X. Yuan, and X. X. Zhu, "Universal domain adaptation for remote sensing image scene classification," *IEEE Trans. Geosci. Remote Sens.*, vol. 61, 2023, Art. no. 4700515.

[8] J. Zheng et al., "Open-set domain adaptation for scene classification using multi-adversarial learning," *ISPRS J. Photogramm. Remote Sens.*, vol. 208, pp. 245–260, Feb. 2024.

[9] J. Zheng, Y. Zhao, W. Wu, M. Chen, W. Li, and H. Fu, "Partial domain adaptation for scene classification from remote sensing imagery," *IEEE Trans. Geosci. Remote Sens.*, vol. 61, 2023, Art. no. 5601317.

[10] Y. Zhang, W. Li, M. Zhang, Y. Qu, R. Tao, and H. Qi, "Topological structure and semantic information transfer network for cross-scene hyperspectral image classification," *IEEE Trans. Neural Netw. Learn. Syst.*, vol. 34, no. 6, pp. 2817–2830, Jun. 2023.

[11] J. Zheng et al., "Cross-regional oil palm tree counting and detection via a multi-level attention domain adaptation network," *ISPRS J. Photogramm. Remote Sens.*, vol. 167, pp. 154–177, Sep. 2020.

[12] Y. Ganin et al., "Domain-adversarial training of neural networks," *J. Mach. Learn. Res.*, vol. 17, no. 1, pp. 2030–2096, Apr. 2016.

[13] J. Zheng et al., "A two-stage adaptation network (TSAN) for remote sensing scene classification in single-source-mixed-multiple-target domain adaptation (S^2M^2T DA) scenarios," *IEEE Trans. Geosci. Remote Sens.*, vol. 60, 2022, Art. no. 5609213.

[14] B. Fu et al., "Learning to detect open classes for universal domain adaptation," in *Proc. 16th Eur. Conf. Comput. Vis. (ECCV)*, Glasgow, U.K. Cham, Switzerland: Springer, Aug. 2020, pp. 567–583.

[15] J. M. Dolezal et al., "Uncertainty-informed deep learning models enable high-confidence predictions for digital histopathology," *Nature Commun.*, vol. 13, no. 1, pp. 1–14, Nov. 2022.

[16] K. He, X. Zhang, S. Ren, and J. Sun, "Deep residual learning for image recognition," in *Proc. IEEE Conf. Comput. Vis. Pattern Recognit. (CVPR)*, Jun. 2016, pp. 770–778.

[17] M. Long, Y. Cao, J. Wang, and M. Jordan, "Learning transferable features with deep adaptation networks," in *Proc. 32nd Int. Conf. Mach. Learn.*, vol. 37, Jul. 2015, pp. 97–105.

[18] M. Long, H. Zhu, J. Wang, and M. I. Jordan, "Deep transfer learning with joint adaptation networks," in *Proc. Int. Conf. Mach. Learn.*, 2017, pp. 2208–2217.

[19] M. Long, Z. Cao, J. Wang, and M. Jordan, "Conditional adversarial domain adaptation," in *Proc. 32nd Int. Conf. Neural Inf. Process. Syst.*, 2018, pp. 1647–1657.

[20] K. You, M. Long, Z. Cao, J. Wang, and M. I. Jordan, "Universal domain adaptation," in *Proc. IEEE/CVF Conf. Comput. Vis. Pattern Recognit.*, 2019, pp. 2720–2729.

[21] K. Saito, D. Kim, S. Sclaroff, and K. Saenko, "Universal domain adaptation through self supervision," in *Proc. Adv. Neural Inf. Process. Syst.*, vol. 33, 2020, pp. 16282–16292.

[22] K. Saito and K. Saenko, "OVANet: One-vs-all network for universal domain adaptation," in *Proc. IEEE/CVF Int. Conf. Comput. Vis. (ICCV)*, Oct. 2021, pp. 9000–9009.

[23] W. Chang et al., "Unified optimal transport framework for universal domain adaptation," in *Proc. Adv. Neural Inf. Process. Syst.*, vol. 35. Red Hook, NY, USA: Curran Associates, 2022, pp. 29512–29524.

[24] G.-S. Xia et al., "AID: A benchmark data set for performance evaluation of aerial scene classification," *IEEE Trans. Geosci. Remote Sens.*, vol. 55, no. 7, pp. 3965–3981, Jul. 2017.

[25] G. Cheng, J. Han, and X. Lu, "Remote sensing image scene classification: Benchmark and state of the art," *Proc. IEEE*, vol. 105, no. 10, pp. 1865–1883, Oct. 2017.

[26] Y. Yang and S. Newsam, "Bag-of-visual-words and spatial extensions for land-use classification," in *Proc. 18th SIGSPATIAL Int. Conf. Adv. Geograph. Inf. Syst.*, Nov. 2010, pp. 270–279.